

CALORIMETRY UNDER STRESS

A preliminary study in single crystalline Cu-Zn-Al shape memory alloys

J. L. Pelegrina¹, M. Sade², C. Auguet³, V. Torra^{3} and A. Torralba³*

¹CONICET, Metals Division, Centro Atómico, 8400 S. C. de Bariloche

²Metals Division, Centro Atómico, 8400 S. C. de Bariloche, Argentina

³CIRG-DFA-ETSECCPB-UPC Campus Nord, B-4, E-08034 Barcelona, Spain

Abstract

A non-differential calorimetric analyzer was developed for an INSTRON 1123 machine (a stress-strain-temperature analyzer) with a temperature chamber INSTRON 1110. The study was performed using the Joule effect and pseudoclastic martensitic transformations in single crystals of Cu-Zn-Al alloys. The analysis of the system establishes that: the sensitivity of calorimetric measurements after a filter of two poles and two zeros is 166 mV W^{-1} (at 297 K), the noise is near $1.5 \text{ } \mu\text{V}$ and the drift is close to $30 \text{ } \mu\text{V}$ in 6 h. The reproducibility of the sensitivity working with one sample is better than $\pm 0.3\%$, and the change to a new sample keeps the value below $\pm 0.5\%$. The uncertainty in reproducibility in the martensitic transformation (including repositioning) does not overcome $\pm 1.6\%$. The used calorimetric sensors limit the temperature to 373 K. The furnace control originated fluctuations on the base line (near $\pm 20 \text{ } \mu\text{V}$), which by means of an auxiliary signal processing were reduced to 50% (less than $\pm 10 \text{ } \mu\text{V}$).

Keywords: martensitic transformation, noise suppression, non-differential conduction calorimetry, phase transition, single crystal, signal processing

Introduction

The martensitic transformation in Cu-based alloys is a transition between metastable phases [1]. It can be induced by a change of temperature and/or by the application of appropriate stresses. The martensitic transformation of the β phase of Cu-Zn-Al alloys has been measured using conventional and non-conventional calorimeters (DSC and/or conduction calorimeters) [2-4]. The quantitative measurements, which this technique allows, have shown to be useful for a better understanding of the behaviour of these shape memory alloys [5, 6].

The calorimetric analysis of temperature induced martensitic transformation (stress free), although being the main use of calorimetric measurements, implies a high complexity of the transition path. The appearance of several variants and,

* Author to whom all correspondence should be addressed.

within each one, of a great number of plates, produces an increase of the temperature range of the transformation due to the internal stresses created by their interaction. This leads also to an incomplete transformation of the whole mass of the sample. Therefore in most cases, due to the uncertainty in the determination of the exact temperature at which the transformation finishes, the base line of the curve is ill defined and the heat is not well determined. In some cases, an additional uncertainty is present due to the nucleation and growth of more than one martensitic phase which have close free energies. Additionally, the martensitic transformation on Cu-based alloys presents a particular synergetic related to the complexity of the processes associated to the transition. This is mainly explained by the appearance of burst processes, internal stresses inducing local transformation temperature changes, the creation of dislocations, the evolution of the hysteresis cycle, etc. [6, 7]. The aforementioned aspects compel to pay a lot of attention to the interpretation of calorimetric results, if accurate values are desired. It also has induced the development of instrumentation specially adapted to bear with the complexity of the system [8].

It is now clear that the properties of the transformation and of the calorimeters impose a careful analysis of the hypothesis traditionally assumed, and will need an appropriate understanding of reliability in conduction calorimeters. The main difficulties which are found in conduction calorimetry are related to differences and misunderstandings between accuracy, resolution and reproducibility. These difficulties are induced by the intrinsic complexity of conduction calorimetry: it relates irreversible physicochemical phenomena, the heat transfer and the signal processing.

The application of a tensile or a compressive stress, by determining a privileged axis, produces the transformation to a single variant, thus reducing the complexity. This single variant grows generally in multiple domains, and it has been shown that the coalescence of these martensite domains only produces stacking faults. Therefore, the possibility of doing measurements of the dissipated heat in mechanical stress-strain tests is attractive, as it would help to simplify the interpretation of the results. The field of application of such a calorimetric analyzer could include, for instance, the study of plastic deformation (dislocation production), the stress induced phase transformations and the effect of precipitates on several features of the behaviour of materials.

The introduction of calorimetric devices in stress-strain equipment has received some attention in the last few years [9, 10]. The system consisted of a differential calorimeter located in one face of the stressed sample, being the other face in contact with an insulating sheet. This type of experimental device leads to two difficulties:

1. the detector only covers a reduced part of the sample surface;
2. the classical theory of heat transfer in conduction calorimeters was developed for heat sinks of considerable size. In an explicit or implicit form, the classical treatments of calorimeters always include a well defined heat sink with a reference temperature, unaffected by the process or the surroundings. The differential system [10], due to the small distance between reference and measurement sensor can be affected by the analyzed phenomena and, probably, by fluctuations on room temperature. In

addition, direct contact between sample and isolating materials can modify time constants affecting, for instance, the base line.

The aim of this work is to present a new experimental device, developed to make non-differential calorimetric measurements in a commercial mechanical testing machine. Special attention was paid to each step to clarify the origin of the errors acting on the results. Preliminary measurements have been performed using tensile stress induced martensitic transformations of Cu-Zn-Al single crystals. The potential use of this calorimetric device to martensitic transitions will be analyzed considering:

- a) The calorimetric experimental conditions (an open system with non-differential structure).
- b) The reproducibility and errors on the consecutive measurements, for instance in Joule effects as also after the sample replacement (assembly/disassembly).
- c) The expected uncertainties in the transformed material (crystal orientation, other lengths and position of transformed zone) which contribute to the calorimetric signal.
- d) The available tools in signal processing to analyze stepped changes of the base line induced by the transformation, and also, base line fluctuations induced during measurements at temperatures higher than room temperature.

The dependence of the sensitivity with the position and the elongation of the transformed zone will not be taken into account in this work.

Experimental set-up and samples

Two alloys of compositions: Cu - 19.71 at% Zn - 14.15 at% Al and Cu - 15.14 at% Zn - 16.43 at% Al were prepared using metals of purity greater than 99.99%. They had an electron concentration $e/a=1.48$, and a nominal M_s of 145 and 251 K respectively. The alloy with M_s near room temperature was used for the stress induced experiments, whereas the calibration samples were prepared from the other alloy. Two single crystals from each alloy were grown by a modified Bridgman method. Flat samples were prepared with a low speed diamond saw with the following dimensions: total length ≈ 62 mm, width ≈ 7.5 mm and depth ≈ 3 mm. The part where the calorimeter is applied has a length ≈ 20 mm and a width ≈ 4 mm. From each single crystal only one sample was obtained. The crystallographic direction of the sample axes (Table 1) was determined by the Laue method. In order to reduce the possible effects of a change in the thermal contact between the sample and the calorimetric sensor due to the shear produced by the transformation, the face of the samples (M1 and M2) was cut with the shear direction contained in the flat surface. The samples were heat treated at 850°C during 20 min and cooled in air to room temperature. This heat treatment produces bigger martensite plates or the ease growth of only one. The surfaces were then mechanically and electrolytically polished. The calibration samples had the same shape as the transforming ones, but with a hole throughout of ≈ 9 mm length and ≈ 1 mm width. An insulated manganin wire was tightly bound inside the hole, and heat was dissipated using different intensities and times.

Table 1 Values used in the filters: two poles (τ_1) and two zeros (τ_1^*)

$T/$ K	$\tau_1/$ s	$\tau_2/$ s	$\tau_1^*/$ s	$\tau_2^*/$ s
296.9	680	100	550	96
314.4	720	153	590	144
323.1	720	153	590	144

An INSTRON 1123 equipped with a temperature chamber INSTRON 1110 was used as the standard stress-strain-temperature system. A load cell with a maximum capacity of 500 kg was used, which permits a resolution of 0.5 kg. The elongation of the stressed samples was obtained from the crosshead movement, with a resolution of 2 μm . A special grip was used which allows the movement of the sample to reduce the bending forces close to the heads. The samples were tensile stressed at two crosshead speeds: 0.1 and 0.2 mm min^{-1} . The calorimetric measurements during the martensitic transformation were performed for four different elongations (near 0.1, 0.2, 0.3 and 0.4 mm) corresponding to different amounts of transformed phase.

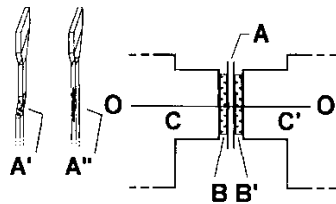


Fig. 1 Sample and calorimetric detectors (schematic distribution). A: sample; A': sample deformation on transformation; A'': resistance position in a hole; B and B': calorimetric detectors (MELCOR); C and C': reference copper blocks; O-O': calorimetric axis

The calorimetric system shown in Fig. 1 is composed of two symmetric elements each formed by a MELCOR thermoelectric sensor FC0.6-66-05L (B and B') and a copper block (C and C') used as an independent heat sink. Platinum resistances in C and C' measure the reference temperatures $T_1(t)$ and $T_2(t)$ respectively. The elements are in contact with the two opposed surfaces of the sample (A). In this way heat is transferred to the two thermobatteries simultaneously and to the grips. The curve is the sum of signals produced by the MELCOR sensors. Two horizontal steel bars serve as guidelines to the proper alignment of the calorimetric axis O-O', and provide for the reproducible assembly of the system. In each steel bar, a spring warrants a minimum compression against the sample, maintaining in this way the thermal contact between the elements and the sample. A little bit of APIEZON L grease stabilizes the thermal resistance in each surface. The calorimetric system is supported by means of a flat surface fixed to the lower grip of the tensile machine. In addition, the whole device is completely free to move horizontally on six steel balls distributed under the Cu blocks. This movement capability allows the grip adaptation under

the application of the external stress. The stress induces a displacement of the bottom grip, and as a consequence the relative position between sample and MELCOR sensors evolves roughly a half of the global displacement. The relative movement differs between elastic and transformation strain. The former is a minor effect affecting the complete deformation length and the latter only appears as a local effect. In the elastic part of the analysis (without phase transformation) or in the transformation path, some little frictional displacement is expected on the sample and a minor quantity of exothermic heat is measured.

Results and discussion

Calorimetric output: signal processing methods and results

The calibration procedure uses Joule effects on resistances. Two different samples with a similar hole (or resistance position) were used. The target was to evaluate the effect of sample preparation (cutting, polishing, etc.) and positioning. The wires (manganin or constantan) are put inside a 9 mm hole situated perpendicular to the calorimetric axis (A'' in Fig. 1). The PC-computer (via a QUICK-BASIC program) controls the independent readings of four DMM (two signals from the MELCOR sensors and two temperatures from C and C' in Fig. 1) and establishes the on/off signals in a Keithley power supply to generate the Joule effects. In this work, the sampling used (Δt) is 0.8 s. The dynamic performances of the system are evaluated using inverse filtering. The experimental observations indicate that the values of the poles and of the zeros obtained via inverse filter (Table 1) are similar (± 5 s) for all the analyzed samples. This coincidence indicates a good similarity of the complete set of samples (for calibration and transformation measurements) at the dynamic scale, including the rebuilt of the system with the same sample or with a different one. The limited increase of the parameters with the temperature is coherent with other observations of calorimetric systems [11].

The signal processing uses two steps

The first one is an eventual smooth of furnace effects (above room temperature) realized separately for each part of the detector system [8, 12]. At higher temperatures the furnace induces fluctuations in temperature (near ± 0.3 K) and on base line ($T_1(t)$, $T_2(t)$ and $s(t)$ in Fig. 2). Noise reduction is performed working via linear regression between the calorimetric noisy signal $s'(t)$ and the reference signal $r(t)$ which was obtained by the platinum resistance in C and C' (Fig. 1). The model is

$$s'(t) = ar(t) + b \quad (1)$$

being $s'(t)$ the part of the calorimetric signal due to the ambient perturbation (thermostating effects) and $r(t)$ the resistance. The signal with noise reduction $s''(t)$ is defined as

$$s''(t) = s(t) - s'(t) \quad (2)$$

The parameters a and b are estimated by minimizing the squared error between $s(t)$ and $s'(t)$ in a time interval where variations in $s(t)$ are only due to ambient temperature variations (without Joule or external stressing effects). In Fig. 2 two examples are presented. The curve $s(t)$ (the sum of the signals of the left and right sensors of Fig. 1), after the independent temperature correction, smooths to $s_c(t)$. Figure 2 clearly shows that a background fluctuation remains after correction. The developed algorithm only acts on the effects directly related to the oscillation of temperature inside the furnace (higher frequencies). It doesn't consider the effect of temperature fluctuations of lower frequencies. Although the linear regression does not take into account a more complex model including a transfer function between noise and reference signal, this simple method reduces noise to near 25% of the original value.

The second step is the calorimetric curve transformation to useful parameters.

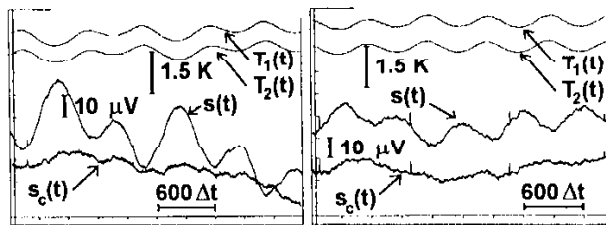


Fig. 2 Furnace noise suppression. $s(t)$: experimental calorimetric curve, $s_c(t)$ after noise reduction. Left: sample used in Joule analysis (314.4 K); right: sample used in transformation analysis (315.6 K)

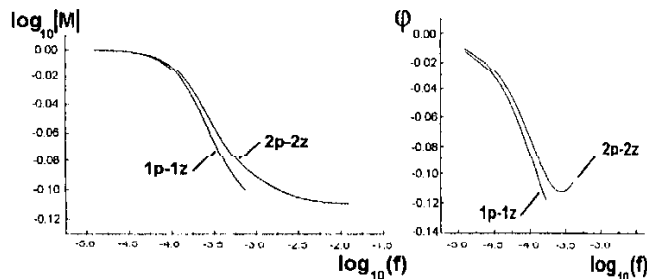


Fig. 3 Left: modulus vs. frequency; right: phase (at 296.9 K)

The base line correction uses a linear fit before the Joule effect or the load process. After base line determination, a deconvolution of each curve is performed using inverse filtering (Table 1 the used filters). Figure 3 shows that dynamic effects of the used filters are not highly relevant in comparison with the filter effect using only one pole and one zero. The presence of zeros (inside the pole series) produces a completely different behaviour as compared to the classical calorimeters, for instance, those similar to the Tian-Calvet (mainly poles). The dynamic analysis of a theoretic

cal model developed for the present equipment, with detection near the dissipation, always contains a zero located between each pole pair.

From calorimetric curve to sensitivity (Joule effects)

The Joule effect doesn't induce any change on the position of the sample. It allows to subtract the base line and to carry out the calculation of the sensitivity (S_{ens}) defined by the area under the calorimetric curve divided by the energy given in the Joule effect. Several independent series (or 'sets') of Joule effects were made. In each set several Joule effects are produced without any change on the experimental system. Between each set of measurements, a disassembly and a rebuilt of the system has been performed, with an eventual change of the sample. In Table 2 are shown the resistances used in the Joule effect.

Table 2 Samples used to calibrate the system and the corresponding resistance

Sample	R/Ω
J1	63.42
J2	8.816

In Tables 3 and 4 the averages of the sensitivities are presented. Table 3 corresponds to the room temperature with three sets of measurements. For each series of successive Joule effects the dispersion is inferior to 0.3%. The assembly and disassembly effects including change of the sample maintain the error below 0.5%.

Table 3 Sensitivity (S_{ens}) at ambient temperature: 296.9 (without furnace effects). Filter using 2 poles and 2 zeros. Samples used J1 and J2. N: number of Joule measurements in each set. σ standard deviation

Set	Sample	N	$S_{\text{ens}}/\text{mV W}^{-1}$	$\sigma/\text{mV W}^{-1}$	Relative error/%
1	J1	10	165.8	0.5	0.28
2	J1	10	167.0	0.4	0.22
3	J2	6	165.2	0.3	0.17
Mean	value	26	166.1	0.8	0.48

Table 4 Sensitivity (S_{ens}) in mV W^{-1} at higher temperatures for sample J2. With (A) and without (B) furnace noise. Only one set at each temperature. N is the number of runs in each set

T/K	N		$S_{\text{ens}}/\text{mV W}^{-1}$	$\sigma/\text{mV W}^{-1}$
314.4	8	A	171.2	0.9
		B	170.9	0.3
323.1	8	A	172.1	0.4
		B	172.1	0.4

Table 4 corresponds to a preliminary analysis at two higher temperatures. In this case sample J2 was used without analyzing the effect of the assembly/disassembly [13]. The fluctuation of the base line induced by the effects of the furnace introduces a bigger uncertainty and it affects the results. The correction of the temperature effect of the furnace maintains the error below 0.5% (without disassembly).

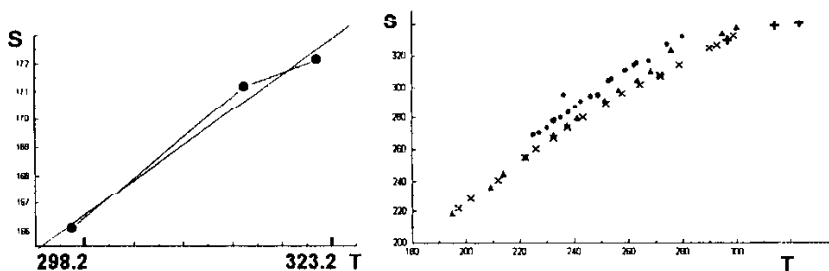


Fig. 4 Left: Sensitivity vs. temperature. Right: Classical sensitivity (S in mV W^{-1}) vs. temperature (T in K) using a non-conventional conduction calorimeter using different heaters Δ , \circ , \times and relative values in this work (+)

Figure 4 (left) shows the dependence of the sensitivity vs. temperature. Figure 4 (right) indicates that, in relative scale, the evolution of $S_{\text{ens}}(T)$ is close to the classical values, obtained for the non conventional system [14].

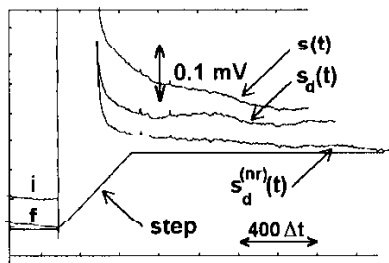


Fig. 5 Filtering effects. $s(t)$: calorimetric curve; $s_d(t)$: calorimetric curve after deconvolution; $s_d^{(nr)}(t)$: calorimetric curve after furnace noise reduction and deconvolution; step: base line step correction related to strain effect; i: initial position of the calorimetric curve; f: initial position of calorimetric curve after complete processing

An approach to the base line of the transformation thermograms

A change on the base line level is produced after each change of applied stress. Two different effects are considered: the elastic elongation and the contribution of the transition. The change of base line level takes place due to the relative displacement between the sample and the calorimetric sensors. The effect is associated to the existence of a vertical distribution of the temperature induced by the interaction of the room temperature on the external axis and grips of the INSTRON machine. A first approach

suggests that the modification of the position (and of the local temperature) induces the base line change by means of a convolution. It is considered that this convolution uses the same transfer function that the Joule dissipation or the transformation itself. The elongation taking place in the INSTRON machine is linear with time. We can consider then that after the deconvolution the previous slope of base line is recovered but the line is displaced. To connect the two straight lines a segment is built (step in Fig. 5) during the time in which the elongation takes place: A straight line links the left base line (previous) to the right base line (after transformation). The numeric treatment allows to visualize the frictional effects of the relative movement on the elastic part (e in Fig. 6), the thermogram shape and the dissipation associated to the transformation (s and s_d in Fig. 6).

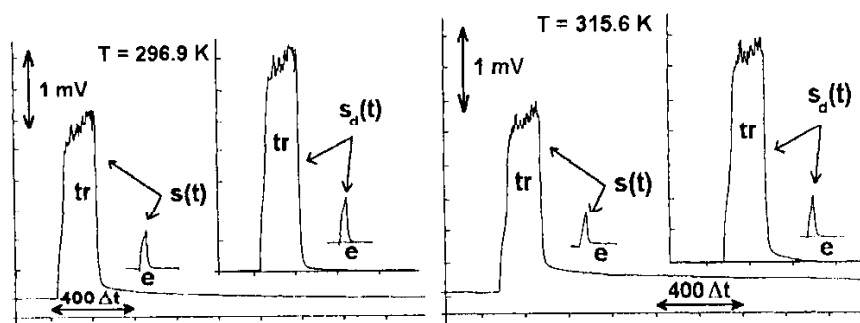


Fig. 6 Transformation calorimetric curve $s(t)$ and deconvoluted curve $s_d(t)$; e: 'elastic' calorimetric curve (without transformation) Left: at 'room' temperature (296.9 K); right: at 315.6 K (after furnace noise reduction)

Crystallographic and geometric analysis for the mass evaluation

The mass of the transformed region was evaluated from the measured deformation Δl . For a transformation that can be described as a simple shear γ , the strain ϵ is given by [15]

$$\epsilon = \frac{\Delta l}{l_0} = \gamma \cos \Phi \cos \lambda \quad (3)$$

with the angles defined relative to the tensile axis. Φ is the angle of the invariant plane normal (habit plane) and λ is the corresponding to the shear direction. The shear γ can be deduced from the phenomenological theory of martensitic transformations and therefore the initial length l_0 of the transformed volume is obtained. The corresponding mass is

$$m = \rho V = \rho a b l_0 = \frac{\rho a b \Delta l}{\gamma \cos \Phi \cos \lambda} \quad (4)$$

with ρ the density of the alloy and a (b) the width (thickness) of the sample.

The accuracy of the method to evaluate the enthalpy of transformation is limited by the error in the determination of the mass. Each term in Eq. (4) will be analyzed under the better conditions. The density of the alloy can be measured with a sample in the form of a parallelepiped or a cylinder, obtaining values with uncertainties of the order of 1 in 10^3 . The shape of the sample can be given with high precision tools, and an error in width and thickness as low as 0.01 mm can be obtained. The elongation Δl was determined from the graphic recorder of the INSTRON machine, and an error of 0.2 mm in the paper (0.002 in the sample) was estimated. In order to avoid an unnecessary increase in the error, the transformation should be followed until an elongation of 0.2 mm or higher is reached. This value could be reduced if an extensometer were used. The shear γ is calculated from the tetragonal distortion, using the relation of the latter with the transformation temperature M_s [1]. By supposing an uncertainty in M_s of 5 K, a relative error in the shear of 3 in 10^3 is obtained. The last product of the two trigonometric functions is generally known as the Schmid factor. Assuming that the back reflection Laue method allows the determination of the tensile axis with a scatter of 2° , a cone of directions 2° around the measured axis was used to evaluate this factor. The standard deviation of this set of values is 4%. Then, the relative error of the mass is mainly due to the impossibility to determine the tensile axis (and as a consequence the transformed volume) with a better accuracy.

Analysis of preliminary transformation results

We have performed several sets of observations with the sample M1 and some measurements with sample M2. The load process has been carried out in two stages, a first one in the elastic range and a second one associated to the pseudoelastic transition. The characteristic parameters of the samples M1 and M2 undergoing the martensitic transformation are shown in Table 5, including the amount of transformed material as a function of elongation.

Table 5 Samples used for the martensitic transformation, density: ρ , width: a , thickness: b , transformation shear: γ , and transformed mass per unit elongation

Sample	Tensile axis	Schmid factor	$\rho/\text{g cm}^{-3}$	a/cm	b/cm	γ	$m/\Delta l/\text{g cm}^{-1}$
M1	[6 7 16]	0.396	7.691	0.400	0.303	0.192	12.2604
M2	[7 17 20]	0.344	7.691	0.396	0.287	0.192	13.2348

A small exothermic signal (e in Fig. 6) has been observed in the elastic range. Once a stable base line is obtained, an increase in load induces the transformation. In Table 6 the relative values of the area of the calorimetric curves (the 'elastic' part was subtracted) have been tabulated. Also shown are the measured elongation, the speed of deformation and the calculated entropy in relative units (see below). This table corresponds to the observations (sample M1) at room temperature. It is observed that the results after a complete disassembly of the sample maintain a satisfactory reproducibility near 1%. The Table 8 contains similar results for the sample

M2 and the results from the sample M1 corresponding to higher temperature. All the results obtained to the room temperature (samples M1 and M2) have been represented in Fig. 7. The difference between both samples are related to the tensile axes and to the uncertainties in its dimensions.

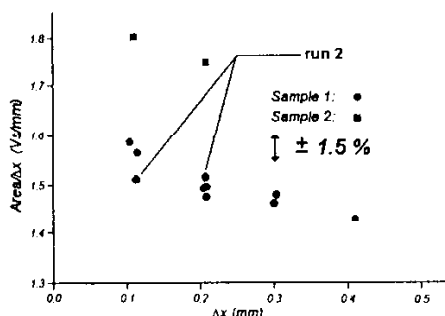


Fig. 7 Positioning uncertainty effect vs. the transformation elongation

Observations of the critical transformation stress against temperature establishes that the transition entropy is independent of the temperature [1]. Thus an analysis of the entropy change was chosen to analyze the coherency of the results using only sample M1. In the experimental measurements the transformed area is, at most, a half of the domain occupied by the resistances used to analyze the Joule behavior. Also, in the hypothesis that the transformation is carried out in the center of the sample, the sensitivity of the system should decrease if larger deformations were used (as indicated by the models based on the RC analogy). In Fig. 7 a progressive decrease of the area of the calorimetric curve per unit deformation as a function of the

Table 6 Transformation results after filtering for sample M1 at room temperature

Measurement	Relative area/ Vs mm ⁻¹	Δx / mm	Speed/ mm min ⁻¹	ΔS / arbitrary units
M1-01	1.4770	0.2080	0.1	2.99
M1-02	1.4651	0.3000	0.1	2.97
M1-03	1.5855	0.1035	0.1	-
M1-04	1.5649	0.1135	0.2	-
M1-05	1.5156	0.2065	0.2	3.07
M1-06	1.4817	0.3030	0.2	3.00
M1-07	1.4333	0.4100	0.2	-
M1-08	1.4942	0.2040	0.1	3.03
M1-09(*)	1.4973	0.2080	0.1	3.03
M1-10(*)	1.5108	0.1120	0.1	-

(*) Performed after a complete disassembly

Table 7 Transformation results after filtering for sample M2 at room temperature, and furnace noise suppression at higher temperature for sample M1

Measurement	Temperature/ K	Relative area/ Vs mm ⁻¹	Δx / mm	Speed/ mm min ⁻¹	ΔS / arbitrary units
M2-01	296.9	1.7456	0.2070	0.1	–
M2-02	296.9	1.8028	0.1080	0.1	–
M1-11(*)	315.6	1.6102	0.2120	0.1	2.99
M1-12(*)	315.6	1.6195	0.2105	0.1	3.01
M1-13(*)	321.5	1.7389	0.2130	0.2	3.14
M1-14(*)	321.6	1.7927	0.2080	0.2	3.24
M1-15(*)	321.5	1.7628	0.1140	0.1	–
M1-16(*)	321.6	1.7050	0.2070	0.1	3.08

(*) Performed after a complete disassembly

elongation can be observed. In Tables 6 and 7 the values of ΔS have been calculated in arbitrary units using

$$\Delta S = \left[\frac{\left(\sum s(t_i) \Delta t \right)_1}{\Delta x S_{\text{ens}}} \right] T \quad (5)$$

Only the values corresponding to elongations of 0.2 and 0.3 mm were calculated as suggested from Fig. 7. For this, it has been used a linear approach to the sensitivity (Fig. 4 left). It is supposed that the elongation is proportional to the mass and that the sensitivity S_{ens} has the same dependence with temperature, independent of the dissipation place. The mean value of ΔS , including the effect of the temperature and of the assembly and disassembly is satisfactory: it only presents a relative error, associated to the standard deviation, of 2.5%.

Conclusions

A device that allows simultaneous measurements of evolved heat and applied stress was developed. The obtained results indicate that this calorimetric system is suitable to analyze martensitic transitions. Relevant features of this open calorimeter can be summarized as follows:

- The performed reduction of the furnace noise allowed to make calorimetric measurements above room temperature.
- Reproducibility of the calibration Joule effects after the rebuilt of the system (as also by changing the sample) is excellent (near 0.5%).
- The proposed method for the correction of the base line showed to be adequate for the evaluation of the calorimetric curve area.

– The heats of transformation have a satisfactory reproducibility with uncertainty near 1.5% if the transformed strain overcomes 0.2 mm.

– The performance as a function of temperature was checked using the entropy change associated to the martensitic transformation.

Further research is needed to improve the accuracy, paying special attention to the sensitivity dependency on the place of heat production (heater position in Joule effects). Also, the sample preparation should allow a precise localization of the transformed zone.

Hint: Identification via a physical image seems an appropriate tool to be used in the correct localization of the transformed zone.

* * *

Mr. Carlos Gómez made the single crystals used in this work. Mr. Carlos Eggenschwiller constructed the calorimetric device.

References

- 1 M. Ahlers, *Prog. Mater. Sci.*, 30 (1986) 135.
- 2 H. Tachoire, J. L. Macqueron and V. Torra, *Thermochim. Acta*, 105 (1986) 333.
- 3 F. H. Tachoire and V. Torra, *Can. J. Chem.*, 67 (1989) 983.
- 4 V. Torra and H. Tachoire, *J. Thermal Anal.*, 36 (1990) 1545.
- 5 J. L. Pelegrina and M. Ahlers, *Acta Metall. Mater.*, 40 (1992) 3221.
- 6 V. Torra and H. Tachoire, *Thermochim. Acta*, 203 (1992) 419.
- 7 H. Tachoire and V. Torra, *Thermochim. Acta*, 266 (1995) 239.
- 8 A. Amengual and V. Torra, *J. Phys. E: Sci. Instrum.*, 22 (1989) 433.
- 9 J. Ortín, L. I. Mañosa, C. M. Friend, A. Planes and M. Yoshikawa, *Phil. Mag. A*, 65 (1992) 461.
- 10 C. J. Elvidge and C. M. Friend, *J. Phys. IV, Supp. J. Phys.*, III 5 (1995) C8-191.
- 11 J. Ortín, V. Torra and H. Tachoire, *Thermochim. Acta*, 121 (1987) 333.
- 12 J. Lerchner, G. Wolf, A. Torralha and V. Torra, *Thermochim. Acta*, 302 (1997) 201.
- 13 F. Marco, Ph. D. Thesis, Univ. of Barcelona 1974.
- 14 C. Auguet, Ph. D. Thesis, Univ. of Barcelona 1987.
- 15 J. W. Christian, *Met. Trans.*, A13 (1982) 509.